Low-frequency noise in n-channel metal-oxide-semiconductor field-effect transistors undergoing soft breakdown

Ming-Jer Chen, Ting-Kuo Kang, Yuan-Hwa Lee, Chuan-Hsi Liu, Yih J. Chang, and Kuan-Yu Fu

Citation: Journal of Applied Physics **89**, 648 (2001); doi: 10.1063/1.1333029
View online: http://dx.doi.org/10.1063/1.1333029
View Table of Contents: http://scitation.aip.org/content/aip/journal/jap/89/1?ver=pdfcov
Published by the AIP Publishing

Low-frequency noise in *n*-channel metal-oxide-semiconductor field-effect transistors undergoing soft breakdown

Ming-Jer Chen,[a] Ting-Kuo Kang, and Yuan-Hwa Lee
Department of Electronics Engineering, National Chiao-Tung University, Hsin-Chu, Taiwan, Republic of China

Chuan-Hsi Liu, Yih J. Chang, and Kuan-Yu Fu
United Microelectronics Corporation, Science-Based Industrial Park, Hsin-Chu, Taiwan, Republic of China

(Received 11 July 2000; accepted for publication 22 October 2000)

For 3.3-nm thick gate oxide *n*-channel metal-oxide-semiconductor field-effect transistors subject to a stress gate voltage of 5.5 V, three distinct events are encountered in the time evolution of the gate current: stress-induced leakage current (SILC), soft breakdown (SBD), and hard breakdown (HBD). The localization of SBD and HBD paths, as well as their developments with the time, is determined electrically, showing random distribution in nature. At several stress times, we interrupt the stressing to measure the drain current low-frequency noise power S_{id}. As expected, S_{id} follows up the spontaneous changes at the onset of SBD and HBD. The S_{id} spectra measured in fresh and SILC mode are reproduced by a literature model accounting for the carrier number and surface mobility fluctuations in the channel, and, as a result, both preexisting and newly generated trap densities are assessed. The post-SBD S_{id} does originate from current fluctuations in the SBD percolation paths, which can couple indirectly to drain via underlying channel in series, or directly to drain if the SBD path is formed close to drain extension. In particular, a fluctuation in S_{id} itself in the whole SBD duration is observed. This phenomenon is very striking since it indeed evidences the dynamic percolation origin concerning the trapping–detrapping processes in and around the SBD paths. The subsequent HBD duration remarkably features a flat S_{id}, indicating the set-up of a complete conductive path prevailing over the trapping–detrapping processes. © *2001 American Institute of Physics.* [DOI: 10.1063/1.1333029]

I. INTRODUCTION

Soft breakdown (SBD), also called B-mode stress-induced leakage current (SILC) (Ref. 1) and quasibreakdown,[2] is currently a highly challenging issue in metal-oxide-semiconductor field-effect transistors (MOSFETs) having ultrathin (<5 nm) gate oxides.[1–7] Current or voltage fluctuations, as described earlier in Refs. 8 and 9, are a primary highlight of the SBD phenomena reported so far.[4,5,10,11] The trapping–detrapping processes in and around certain SBD percolation paths as the origin of the fluctuation mode are well recognized.[4,5,8–11] In particular, the dynamic percolation model[12] advances in-depth understandings.[13] Among many conventional schemes, the low-frequency noise of gate current exhibits the ability of very sensitively detecting the spontaneous changes due to SBD.[5] On the other hand, the drain current low-frequency noise power S_{id}, a measure of the fluctuation of the drain current in the frequency domain, traditionally serves as monitor of the hot carrier robustness and probe of the oxide traps.[14–17] The associated mechanism is well defined in terms of the carrier number and surface mobility fluctuations and a unified, analytic model is built up.[17] However, no extension to the case of soft breakdown is carried out yet. A coupling theory[5] is recently proposed by relating post-SBD S_{id} to current fluctuations in the SBD percolation paths; however, experimental evidence is lacking and the effect of the SBD-path location is not fully clarified. Very recently, the fundamental differences and similarities between SBD and HBD attract much attention;[18–21] however, no comparisons on low-frequency noise are performed.

The aim of this study is to explore the merits of S_{id} characterization while undergoing soft breakdown, with which current understandings concerning the origins of SILC, SBD, and HBD can all be substantially improved. First of all, the localized SBD and HBD paths each are determined electrically. This is essential prior to analyzing S_{id} data. Second, the measured S_{id} indeed follows up the spontaneous changes at the onset of SBD and HBD. Third, both preexisting and newly generated trap densities are extracted using pre-SBD S_{id} data. Fourth, the amount of post-SBD S_{id} depends strongly upon the location of the SBD path, confirming the mentioned coupling theory. Fifth, in the whole SBD duration a fluctuation in S_{id} is observed for the first time. This striking phenomenon evidences the so-called dynamic percolation origin. Eventually, a quite flat S_{id} is noticed in the whole HBD duration, significantly different from SBD.

II. EXPERIMENTS

The *n*-channel MOSFETs under study were fabricated in a 0.18 μm process. In this process, the gate oxide was thermally grown in a dilute oxygen ambient, and the polysilicon

[a]Electronic mail: mjchen@rpl.ee.nctu.edu.tw

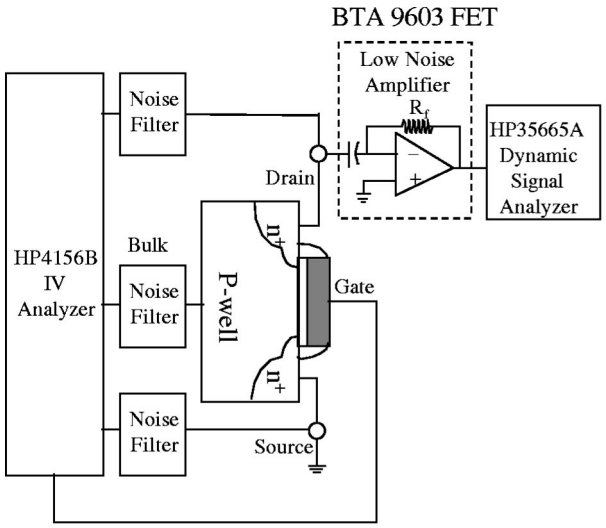

FIG. 1. Schematic diagram of the drain current noise measurement system.

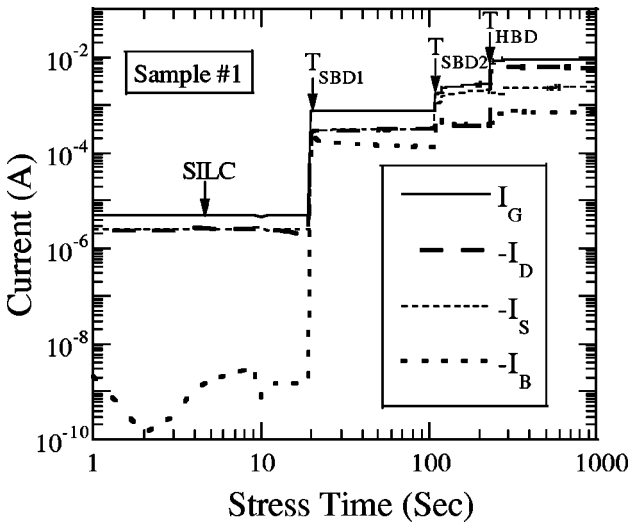

FIG. 2. Measured terminal currents versus stress time under constant voltage stressing for sample #1. The constant voltage of $V_G=5.5\,\mathrm{V}$ is for Fowler–Nordheim (F–N) tunneling stress. There may be a third SBD event quickly following T_{SBD2} due to sudden current change.

gate was arsenic implanted at 50 keV and $2\times10^{15}\,\mathrm{cm}^{-2}$, followed by N_2 and O_2 annealing. The gate oxide size drawn was $10\times10\ \mu\mathrm{m}^2$, and the physical oxide thickness was 3.3 nm as determined by a $C-V$ method accounting for polysilicon depletion and quantum mechanical effects. A constant gate voltage of 5.5 V was adopted to stress gate oxide, with source, drain, and substrate tied to ground. The high-field stressing was interrupted several times for characterization of the threshold voltage V_{th}, the transconductance g_m, and the low-frequency noise power spectrum of drain current. The bias conditions used were (i) $V_D=0.1\,\mathrm{V}$ for drain current vs gate voltage characteristics, from which V_{th} and g_m were extracted above threshold; and (ii) $V_D=0.1\,\mathrm{V}$ and $V_G=1\,\mathrm{V}$ for S_{id} in channel inversion. Figure 1 illustrates the measurement set-up, comprising a HP 35665A dynamic signal analyzer, BTA 9603 FET noise analyzer, and HP 4156B semiconductor parameter analyzer. The measurement frequency ranged from 1 Hz to 1 kHz. Three noise filters were used to eliminate the residual noise in all bias sources. In our work the S_{id} data were the average of the total 20 measurements for each frequency. It was found that S_{id} differs significantly sample by sample.

III. DETAILED RESULTS

A. Sample #1

The evolution of the gate current I_G during constant voltage stressing is depicted in Fig. 2, showing the spontaneous changes as denoted by three critical time points: the time to first SBD $T_{\mathrm{SBD1}}(\approx20\,\mathrm{s})$, the time to secondary SBD $T_{\mathrm{SBD2}}(\approx100\,\mathrm{s})$, and the time to HBD $T_{\mathrm{HBD}}(\approx230\,\mathrm{s})$. The gate current following each of the SBD events exhibits fluctuations as partially magnified in Fig. 3 for $T_{\mathrm{SBD1}}<t<T_{\mathrm{SBD2}}$, while relatively few fluctuations were found not only in the SILC duration (i.e., $0<t<T_{\mathrm{SBD1}}$) but also in the HBD duration ($t>T_{\mathrm{HBD}}$). The current fluctuations in Fig. 3 arise from the trapping–detrapping processes in and around the SBD paths. An analysis of such fluctuations by following the treatments[13] led to the behavior of a non-Gaussian statistical distribution. Also plotted in Fig. 2 are the other terminal currents simultaneously measured, with which the percolation paths can be identified. First of all, the drain current I_D is comparable to the source current I_S in the first SBD duration, indicating that the first-SBD percolation path is located around midchannel, far from source/drain. As to the secondary SBD, a sudden increase is noticed in I_S while I_D is almost unchanged. This suggests that the secondary SBD path appear over the source corner. Eventually, a HBD path is formed close to drain extension as reflected by sudden increase in I_D and unchanged I_S in Fig. 2 for $t>T_{\mathrm{HBD}}$. The corresponding percolation paths are schematically plotted in Fig. 4, where the spheres represent the traps generated during the stress. These paths are drawn based on the recent research[21] on the same oxide thickness; the critical trap number per cell n_{BD} is three for SBD path, while in HBD path n_{BD} is four. In the HBD percolation, the traps spans the

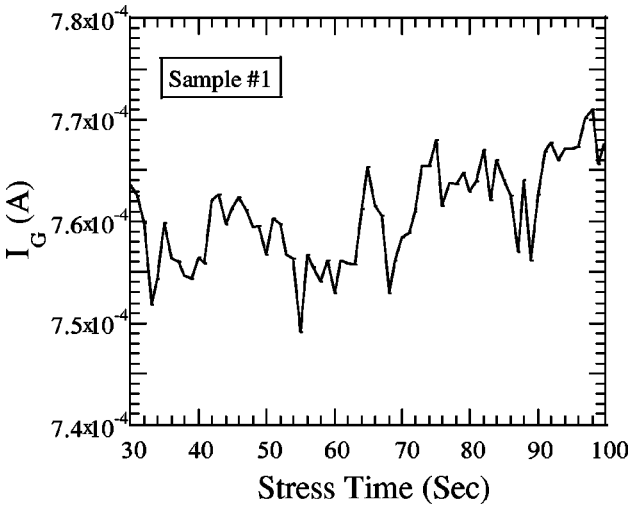

FIG. 3. Detailed evolution of the gate current corresponding to Fig. 2 after the occurrence of the first SBD.

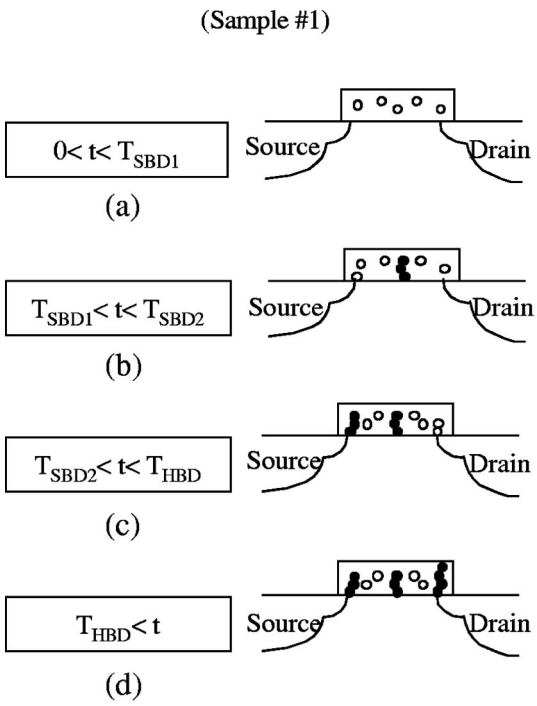

FIG. 4. Schematic cross-section view of the first sample, which shows the SILC mode, the localized SBD paths, and the HBD path, all corresponding to Fig. 2.

whole oxide to connect one plate to the other one, while for the SBD path such plate-to-plate connection is incomplete as characterized by the remaining oxide thickness over the localized physically damaged region (like the shaded spheres in Fig. 4) according to the theory.[2]

The above time to breakdown parameters were defined in terms of sudden increase in gate current. This definition is adequate since it was found that after T_{SBD1} or T_{SBD2} the poststress gate current vs gate voltage characteristic curves resembled the direct tunneling one of the fresh oxide with thinner thickness, whereas it became Ohmic after T_{HBD}. Figure 5 shows the drain current I_D vs gate voltage characteristics monitored at $V_D = 0.1$ V for several stress times. These curves seem to shift toward the positive gate voltage direction with increasing stress time until the catastrophic hard breakdown occurs. This proves the fact that part of the tunneling electrons are trapped in the oxide and the trap number increases with the time. It was found that regardless of SBD, both V_{th} and g_m degradations showed weak dependencies, in agreement with the citation.[5] Figure 6 shows the measured drain current noise power spectrum for different stress times. A view of this figure reveals that S_{id} in the SILC mode increases, then experiencing orders of magnitude increase at the onset of the SBD, again followed by another order of magnitude increase at the onset of the HBD. The post-S_{id} data in some frequency range may be able to fit the $1/f^{\gamma}$ relationship with the power exponent γ very close to unity; however, significant deviations occur for the remaining frequency range. This indicates the existence of the typical Lorentzian spectrum as validated by the aforementioned non-Gaussian distributions deduced from current fluctuations in Fig. 3.

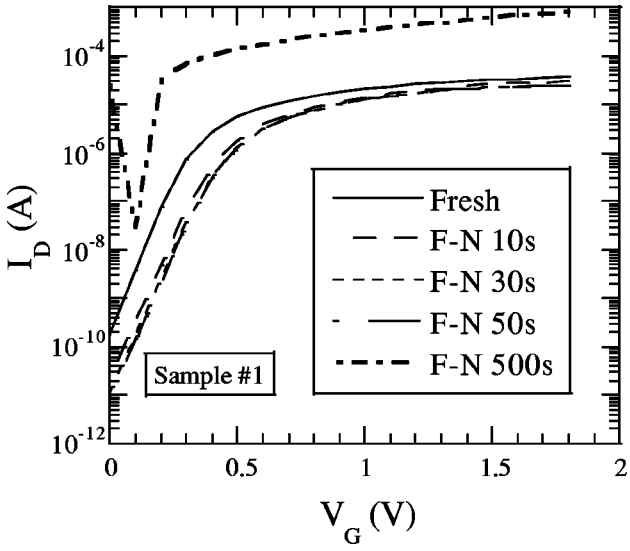

FIG. 5. Measured drain current I_D vs gate voltage V_G curves with $V_D = 0.1$ V for several stress times.

Figure 7 shows the normalization of noise power $(=S_{id}/I_D^2)$ vs the gate current I_G at the same bias condition as the noise measurement. This figure is highly valuable since it exhibits a significant correlation with which S_{id} can be adequately traced to gate current. On the other hand, the S_{id} for a certain measurement frequency can readily follow up the spontaneous changes in gate current during the stressing, as together plotted in Fig. 8. Particularly, two phenomena of concern can be drawn herein. One is the S_{id} fluctuation in the whole SBD duration, looking like a damped sinusoidal waveform. This is the case with high confidence since we have repeated measurements considerably to ensure a smooth and stationary noise spectra. The other is a quite flat S_{id} in the subsequent HBD duration, significantly different

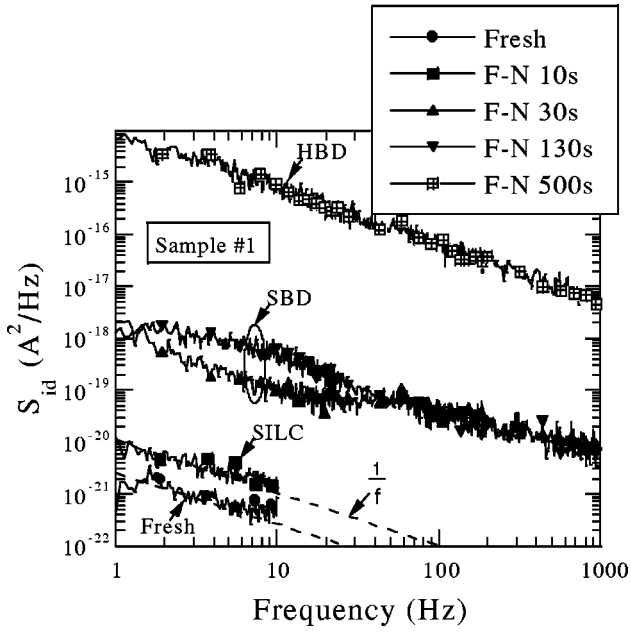

FIG. 6. Measured drain current noise spectra (S_{id}) with $V_D = 0.1$ V and $V_G = 1$ V for several stress times.

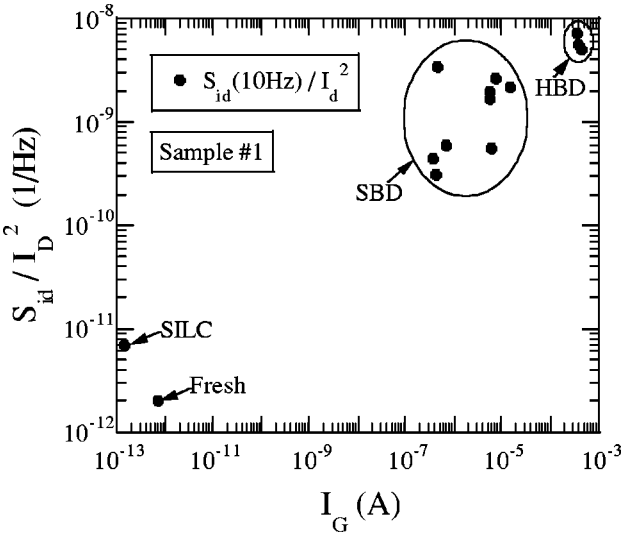

FIG. 7. A correlation plot between normalized drain current noise at 10 Hz frequency and gate current, all from the same bias condition of $V_D=0.1$ V and $V_G=1$ V.

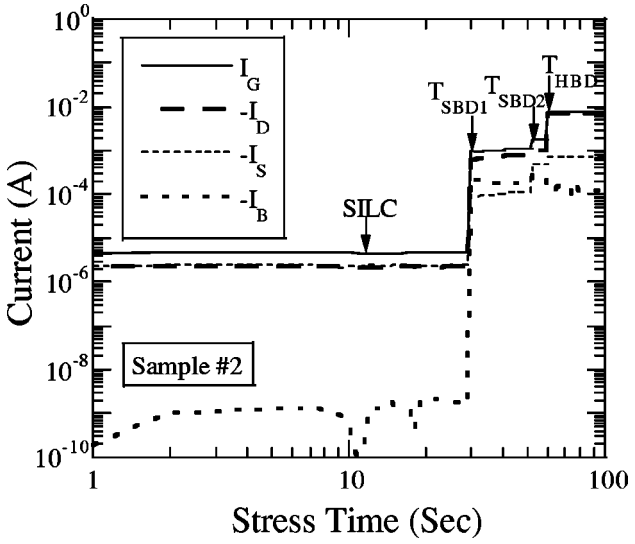

FIG. 9. Measured terminal currents vs stress time under constant voltage stressing for another sample #2.

from SBD. This is consistent with the set-up of a complete conductive path prevailing over the trapping–detrapping processes.

B. Sample #2

Figure 9 shows the evolution of the gate current under the same stress condition for another sample labeled #2, showing the SBD events followed by HBD. The SBD and HBD paths are located accordingly and the results are depicted in Fig. 10. It is argued that the first SBD and the final HBD paths are formed near drain due to sudden rise in drain current, whereas the second SBD path is formed close to source due to sudden rise in source current. Figure 11 shows the measured S_{id} for the first SBD and final HBD along with those from the first sample. It can be seen that the first SBD event of the second sample produces S_{id} about two orders of magnitude larger than the first sample.

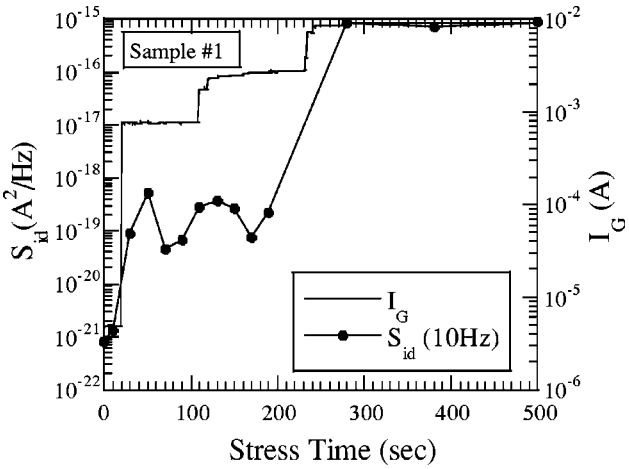

FIG. 8. Measured stress time dependencies of drain current noise at 10 Hz frequency and gate current for comparison. Here the gate current was monitored at $V_G=5.5$ V during the stressing.

IV. ORIGINS OF S_{id}

A. Carrier number and surface mobility fluctuations

The power exponent γ of ≈ 1 for pre-SBD noise data in Fig. 6 indicates that the traps are spatially uniformly distributed within the oxide. The density of the traps responsible, N_T in $\mathrm{cm}^{-3}\,\mathrm{eV}^{-1}$, comprises the pre-existing one N_0 and the newly generated one. Since the latter empirically obeys a power law dependency on the stress time,[22–24] we get explicitly

$$N_T = N_0 + K \times t^{0.5}, \tag{1}$$

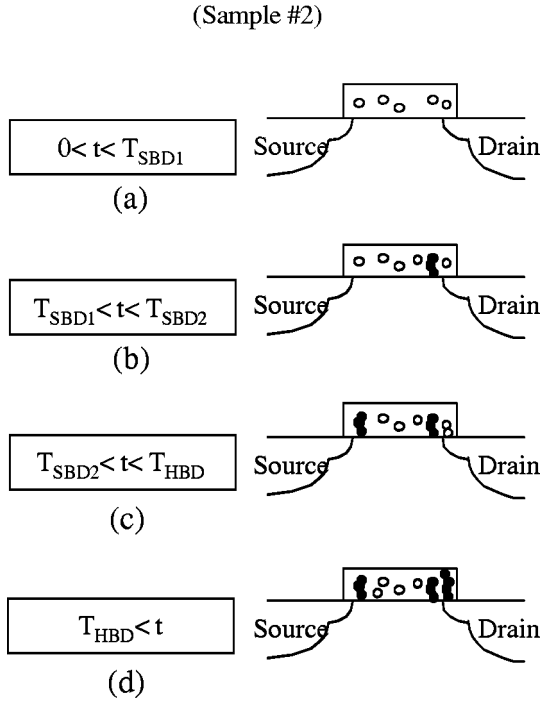

FIG. 10. Cross-section diagrams showing the SILC mode and the localized SBD and HBD paths for another sample #2.

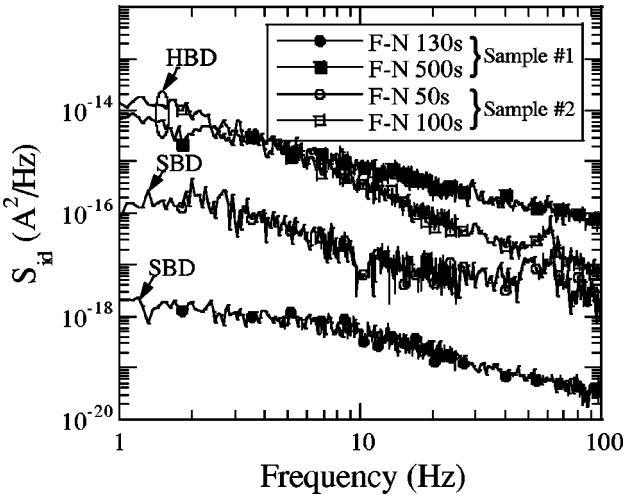

FIG. 11. Comparisons of the measured S_{id} under the bias condition of $V_D = 0.1$ V and $V_G = 1$ V in the first SBD and the final HBD for two samples.

where K is a constant to be fitted. Under the same situation (i.e., uniform distribution for the traps), a unified, analytic model[17] dealing with the carrier number and surface mobility fluctuations can be exactly cited,

$$S_{id} = \frac{kTI_D^2}{\gamma_0 fWL}\left(\frac{1}{N} + \alpha\mu\right)^2 \times N_T, \tag{2}$$

where q is the electron charge; N is the number of channel carriers per unit area; α is the scattering coefficient; μ is the carrier mobility; $\gamma_0 (= 1.29\times 10^8\ \mathrm{cm}^{-1})$ (Ref. 17) is the attenuation coefficient of the electron wave function in the oxide; and W and L are the channel width and length, respectively. We now demonstrate how to extract N_0 and K from fresh and SILC noise data. First of all, the device parameters at $t=0$ as drawn from fresh $I-V$ at $V_D = 0.1$ V in Fig. 5 are $I_D = 2.0\times 10^{-5}$ A, $g_m = 3.0\times 10^{-5}$S, and $V_{\mathrm{th}} = 0.32$ V. μ and N can be straightforward calculated using the formula, $\mu = g_m L/(C_{\mathrm{ox}}\times V_D \times W)$ and $N = (C_{\mathrm{ox}}/q)(V_G - V_{\mathrm{th}} - V_D)$, where C_{ox} is the gate capacitance per unit area. As a result, a fitting to fresh S_{id} data in Fig. 6 produces $N_0 = 5.0\times 10^{16}\ \mathrm{cm}^{-3}\,\mathrm{eV}^{-1}$ for $\alpha = 2.0\times 10^{-15}$ V s. The extracted N_0 respective to used α is reasonable as compared with the reported dependencies.[17] In a similar way, constant K was extracted to be $6.6\times 10^{16}\ \mathrm{cm}^{-3}\,\mathrm{eV}^{-1}\,\mathrm{s}^{-0.5}$ based on S_{id} data at $t = 10$ s.

With known K and N_0, the drain current noise solely due to the carrier number and surface mobility fluctuations can readily be assessed using Eqs. (1) and (2). The amount of the traps increases with the stress until a critical number triggering soft breakdown is encountered. The corresponding traps constitute a percolation path. We assume that outside of the percolation paths, the traps still continue increasing in number with time after SDB events according to Eq. (1). This is valid in nature since essentially the time to soft breakdown parameters such as T_{SBD1} and T_{SBD2} are statistically independent of each other.[18–21] The calculated drain current noise (the input parameters like I_D, V_{th}, and g_m were all from Fig. 5) was found to be negligible respective to SBD data in Fig. 6. This figures out the origin of post-SBD S_{id} far away from the conventional carrier number and surface mobility fluctuations.

B. Current fluctuations in SBD percolation paths

In view of several supporting evidences, we favor gate current fluctuations (see Fig. 3) in the localized SBD percolation paths as the origin of the post-SBD drain current noise; that is, current fluctuations can couple from certain SBD paths through the underlying channel in series, thus bringing noise to the drain. The first evidence is a fluctuation mode in S_{id} in Fig. 8. This phenomenon is possible to elucidate only based on the dynamic percolation model[12,13] or the dynamic trapping–detrapping processes in and around the SBD percolation paths. Also found in Fig. 8 is the second evidence in terms of a flat S_{id} in HBD duration, which can in turn strengthen the first evidence. This is because if the S_{id} fluctuation were not absent in HBD duration, the dynamic percolation origin would not be suitable in SBD duration.

The first SBD S_{id} differs significantly sample by sample as revealed in Fig. 11. This can essentially be traced to the different locations of that SBD path, or equivalently to the presence and absence of the underlying channel in series, respectively. This new finding serves as the third evidence. Two plausible interpretations are presented here. First, in sample #1 the first SBD path is farther from drain and, as a result, the underlying channel in series is resistant to the coupling action, effectively lowering the coupling efficiency. The so-called coupling action is that the trapping and detrapping processes can modulate directly or indirectly the underlying channel potential according to the equivalent circuit published elsewhere.[5] The correlation plot in Fig. 7 can serve as a supporting evidence of this theory. Second, the series channel is bypassed in sample #2 since the first SBD path formed is close to the drain extension, making possible the coupling to affect in a direct manner. No such dramatic differences are found in HBD duration, as expected since the percolation paths responsible are all formed close to the drain.

V. SUMMARY

The localized SBD and HBD paths have been located electrically for *n*-channel MOSFETs undergoing soft breakdown. This enables efficient analyses of S_{id} data. As a result, current understandings concerning the origins of SILC, SBD, and HBD have all been substantially improved. What we have achieved saliently are (i) the S_{id} indeed follows up the spontaneous changes at the onset of SBD and HBD; (ii) the S_{id} data in fresh and SILC mode contain information about the preexisting and newly generated trap densities; (iii) the effect of the SBD-path location is significantly clarified, thus confirming the coupling theory; (iv) a S_{id} fluctuation in the whole SBD duration evidences the dynamic percolation origin; and (v) eventually a quite flat S_{id} in the whole HBD duration points out a complete conductive path dominating.

ACKNOWLEDGMENTS

The authors would like to thank M. J. Chang for performing $C-V$ fitting, and Dr. H. T. Huang and K. N. Yang, Reliability Physics Laboratory, for their stimulating discussions. This work was supported by the National Science Council under Contract No. 89-2215-009-049.

[1] K. Okada, S. Kawasaki, and Y. Hirofuji, Extended Abstracts of 1994 International Conference on Solid State Devices and Materials (SSDM), 1994, p. 565.
[2] S. H. Lee, B. J. Cho, J. C. Kim, and S. H. Choi, International Electron Devices Meeting (IEDM), Tech. Dig., 1994, p. 605.
[3] T. Yoshida, S. Miyazaki, and M. Hirose, Extended Abstracts of 1996 International Conference on Solid State Devices and Materials (SSDM), 1996, p. 539.
[4] M. Depas, T. Nigam, and M. M. Heyns, IEEE Trans. Electron Devices **43**, 1499 (1996).
[5] B. E. Weir, P. J. Silverman, D. Monroe, K. S. Krisch, M. A. Alam, G. B. Alers, T. W. Sorsch, G. L. Timp, F. Baumann, C. T. Liu, Y. Ma, and D. Hwang, International Electron Devices Meeting (IEDM), Tech. Dig., 1997, p. 73.
[6] E. Miranda, J. Suñé, R. Rodriguez, M. Nafria, and X. Aymerich, Appl. Phys. Lett. **73**, 490 (1998).
[7] T. Sakura, H. Utsunomiya, Y. Kamakura, and K. Taniguchi, International Electron Devices Meeting (IEDM), Tech. Dig., 1998, p. 183.
[8] B. Neri, P. Olivo, and B. Ricco, Appl. Phys. Lett. **51**, 2167 (1987).
[9] K. R. Farmer, R. Saletti, and R. A. Buhrman, Appl. Phys. Lett. **52**, 1749 (1988).
[10] T. Tomita, H. Utsunomiya, T. Sakura, Y. Kamakura, and K. Taniguchi, IEEE Trans. Electron Devices **46**, 159 (1999).
[11] F. Crupi, R. Degraeve, G. Groeseneken, T. Nigam, and H. E. Maes, IEEE Trans. Electron Devices **45**, 2329 (1998).
[12] L. M. Lust and J. Kakalios, Phys. Rev. Lett. **75**, 2192 (1995).
[13] N. Vandewalle, M. Ausloos, M. Houssa, P. W. Mertens, and M. M. Heyns, Appl. Phys. Lett. **74**, 1579 (1999).
[14] S. T. Martin, G. P. Li, E. Worley, and J. White, Appl. Phys. Lett. **67**, 2860 (1995).
[15] J. P. Xu, P. T. Lai, and Y. C. Cheng, J. Appl. Phys. **86**, 5203 (1999).
[16] R. Jayaraman and C. G. Sodini, IEEE Trans. Electron Devices **37**, 305 (1990).
[17] K. K. Hung, P. K. Ko, C. Hu, and Y. C. Cheng, IEEE Trans. Electron Devices **37**, 654 (1990).
[18] S. Bruyere, D. Roy, E. Vincent, and G. Ghibaudo, Microelectron. Reliab. **39**, 815 (1999).
[19] E. Wu, E. Nowak, J. Aitken, W. Abadeer, L. K. Han, and S. Lo, International Electron Devices Meeting (IEDM), Tech. Dig., 1998, p. 187.
[20] J. Suñé, G. Mura, and E. Miranda, IEEE Electron Device Lett. **21**, 167 (2000).
[21] M. J. Chen, T. K. Kang, C. H. Liu, Y. J. Chang, and K. Y. Fu, Appl. Phys. Lett. **77**, 555 (2000).
[22] D. J. Dumin, J. R. Maddux, R. S. Scott, and R. Subramoniam, IEEE Trans. Electron Devices **41**, 1570 (1994).
[23] R. Degraeve, G. Groeseneken, R. Bellens, M. Depas, and H. E. Maes, International Electron Devices Meeting (IEDM), Tech. Dig., 1995, p. 863.
[24] M. J. Chen, T. K. Kang, H. T. Huang, C. H. Liu, Y. J. Chang, and K. Y. Fu, IEEE Trans. Electron Devices **47**, 1682 (2000).